



Experiment and Modeling of Milling Force Based on Tool Edge Preparation

XF. Zhao¹ · Y. Yang¹ · L. He^{1,2} · ZG. Feng¹

Received: 20 April 2021 / Accepted: 21 September 2021 / Published online: 7 October 2021
© The Society for Experimental Mechanics, Inc 2021

Abstract

By altering the cutting edge profile, edge preparation can increase the stability of the cutting process, extend the tool life, and improve the machined surface quality. Herein, a theoretical model of cutting force based on milling tool edge preparation is established according to metal cutting theory and material constitutive equations. The influence of edge radius, milling speed, tool feed, cutting depth, and rake angle on the cutting force are investigated. The results of simulations of the tool milling force of a cemented carbide tool milling 45 steel were performed in the metal cutting modeling software AdvantEdge. Theoretical values of cutting force and torque are compared corresponding values obtained through the milling simulations and cutting experiments, respectively, to verify the proposed cutting force model based on edge preparation. The research results provide the basis for realizing the tool edge preparation effect, the high speed and the high efficiency cutting.

Keywords AdvantEdge · Edge preparation · Edge radius · Milling force · Milling torque

Introduction

With the development of high speed, high-precision, and ultra-precision machining, the demand for high-precision cutting tools has grown. Cutting edge preparation can improve cutting performance and workpiece surface quality and prolong tool life by improving the edge morphology [1]. Therefore, studies on the effects of edge preparation on

cutting processes are indispensable. To date, research on the influence of cutting edge preparation has mainly focused on investigating the cutting force, cutting temperature, tool life, and quality of the machined surface through cutting experiments and simulations. The finite element method (FEM) has been widely used to simulate machining processes, and can predict the chip geometry and cutting forces, as well as the temperature and residual stress in the cutting region. Orthogonal cutting is often selected to simplify the modeling process, and empirical, linear, exponential, and polynomial models are typically adopted. However, predictions made by these models are based on the shear, radial, and axial force coefficients of the milling process, whereas the influence of geometric parameters of the milling tool and edge morphology on the cutting force are not considered [2, 3].

To effectively study the strain and force behaviors during metal cutting, predictive analytical models are more economical and more accurate compared to numerical methods and empirical model decomposition. Mark Rubeo used a linear average force model and nonlinear instantaneous force model to show the nonlinear relationship between milling parameters and cutting force coefficients [4]. Jian Weng proposed a semianalytical model to study the effect of chamfered edges on the cutting force considering multiple material flow states. A modified force prediction model was established by introducing factor S to describe changes

Yong Yang, Lin He and Zhiguo Feng contributed equally to this work.

✉ XF. Zhao
zxf801112@163.com

Y. Yang
732311214@qq.com

L. He
helin6568@163.com

ZG. Feng
zgfeng@gzu.edu.cn

¹ Mechanical Engineering College, Guizhou University, Jiaxiu South Road, Huaxi District, Guiyang, 550025, Guizhou, China

² Mechanical Engineering College, Liupanshui Normal University, No. 19, Yucai lane, Minghu Road, Zhongshan District, Liupanshui, 553004, Guizhou, China



in the edge effects with the ratio of chamfer length to uncut chip thickness (UCT). Then, to validate the proposed model, orthogonal cutting experiments were performed using AISI 304 stainless steel as the workpiece and various chamfered carbide inserts [5]. Magalhães presented numerical simulations of hard turning using the FEM to provide a better understanding of mechanical and thermal loads. A higher chamfer angles and larger mechanical load acting on the tool edge are mainly responsible decreasing the tool life [6].

Agmell used the theoretical chip thickness to obtain the cutting forces. The simulated and experimental values showed good correlation. Chamfer effectively reduced the maximal principal stress in the engagement phase since normal forces acting at the chamfer, while the bending of the tool along the axis perpendicular to the simulated plane [7].

Some researches establish the force model considering the edge preparation, mainly focus on the influences of the edge radius on the forces. Zhou et al. presented a novel methodology for predicting micro end-milling cutting forces based on an iterative algorithm. The authors considered the edge radius, material strengthening, and friction coefficient. He showed that the cutting forces increased as the edge radius increases; in addition, varying the friction coefficient affect the cutting force [8].

Fulemova prepared the edges of cutting inserts using grinding, drag finishing, and laser technology and studied the influence of the cutting edge preparation process and cutting edge radius on the tool life, cutting forces, and the roughness of the machined surface [9].

Wang et al. examined the combined effects of cutting edge radius and fiber cutting angle on burr formation. The particular mechanism leading to burr formation in edge trimming of CFRP laminates was investigated, and the influence of fiber cutting angle and cutting edge radius on burr formation were analyzed. Fiber cutting angles were found to be smaller than 90° when a large cutting edge radius was used for both milling and drilling of CFRP composites [10].

Zhu presented a model to investigate the influence of edge radius, tool run-out, flexible deformation, and tool wear on the micro milling force and thoroughly discussed the latest research on micromilling technology and cutting force modeling [11].

Since the tool edge contour prepared is not the circle, whose character parameter is the edge radius. The edge contour are really the asymmetric, whose character parameter is the form factor K . Thus, the influence of the form factor K on the force are investigated. Sauer evaluated the influence of edge radius and form factor K on the thrust force and cutting force during machining of carbon fiberreinforced plastics (CFRP) using an orthogonal cut and proposed a new approach for selecting the optimal parameters of abrasive waterjet cutting for edge preparation.

The analysis revealed that small cutting depths and different cutting edges affect the cutting forces in different edge regions in various ways [12]. Denkena used an abrasive nylon brush to prepare the edge of a physical vapor deposition-coated carbide cutting tool. By changing the contact conditions between the abrasive brush and the workpiece, both a symmetrical edge ($K = 1$) and an asymmetric edge ($K = 2$) could be obtained. The asymmetric cutting edge showed the least wear, whereas a larger cutting force was obtained with the symmetrical cutting edge [13, 14].

A large number of models, including those mentioned above, have been developed to predict the cutting forces in micro end-milling. The effects of edge radius have been considered, which could affect the accuracy of cutting force predictions. The objective of this paper is to present a novel analytical micro end-milling cutting force model, based on the principles of metal cutting and physical properties of materials, that considers the effects of edge radius. The proposed analytical model could contribute to further improvements in the accuracy of cutting force predictions in micro end-milling. Moreover, investigating the influence of edge preparation on cutting forces could also provide more thorough understanding of the micro end-milling process, as well as methods for monitoring cutting force.

In the present study, a novel analytical micro end-milling cutting force model that considers edge preparation and tool geometry was developed. Experiments and FEM simulations were carried out, and the theoretical values were compared with the experimental measurements and simulation results. The FEM model provides a useful way to verify the cutting force theoretical model, and the experimental results validate the theoretical torque model that considers the influence of the edge radius and the cutting parameters. Finally, the effects of edge radius, rake angle, milling speed, and tool feed on the cutting force were investigated using the proposed model. The results provide a useful reference for understanding the effects of cutting edge preparation towards achieving high-speed, high-efficiency machining.

Materials and Methods

Theoretical Model

Cutting force principle with edge radius

Tool edge preparation is the process of turning a less smooth sharp edge of a cutting tool into a smooth predefined shape, usually a rounded edge, to realize highspeed, high-efficiency cutting. Therefore, the edge radius is the main characteristic of the prepared tool edge. The prepared edge



forms a circular arc of radius r_e . Edge radius r_e changes the contact between the rake and the flank cutting surfaces and the workpiece, which affects the cutting force during the cutting process.

In the milling process, the cutting force is mainly composed of the chip forming force on the rake face and the plowing force on the flank face. Friction on the bottom tool edge is small, and can be ignored. The chip forming force is related to the deformation in deformation zone I, friction between the chip deformation and the contact surface, plowing force, flow stress in the workpiece material, and friction conditions of the contact area(CA)surface.

When the edge radius is , the chip forming force and the plowing force are shown in Fig. 1.

Chip forming force model

The milling tool cutting process is depicted in Fig. 2. The chip formation force of the milling tool is affected by the shear force of the rake face. The shear force F_s is related to the chip contact are S_{ABG} , which is determined by the cutting thickness h , radial cutting depth a_e , and spiral angle δ .

According to Fig. 2(a), the cutting thickness of the milling tool h is related to the cutting angle, as follows:

$$h = f_z * \sin \varphi \tag{1}$$

where f_z is the feed engagement (m/z) and φ is the cut-out angle.

Projection of the chip contact area S_{ABG} on a section of the milling tool is illustrated as the shaded area in Fig. 2(b), and its area is S_{ABF} . According to Equation (1), the variation law of the cutting thickness h varies with the cutting angle according to the same principle as the Archimedes spiral thread. Therefore, the area of the

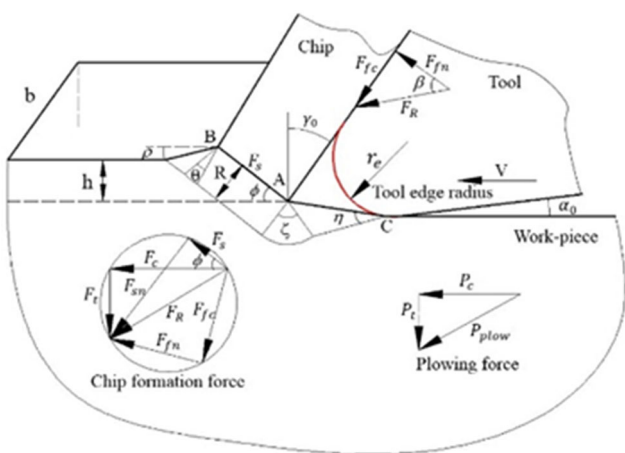


Fig. 1 Cutting forces during chip formation process

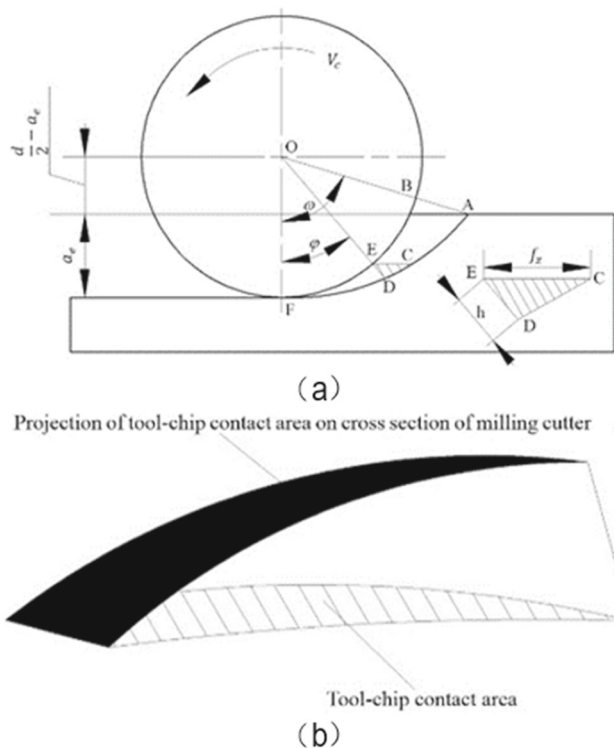


Fig. 2 Cutting process of milling tool: (a) Schematic illustration of milling process; (b) Contact area between milling tool and chip

Archimedes spiral thread can be used to solve the projected area S_{ABF} , expressed as

$$S_{ABF} = \int_0^\omega \frac{1}{2} \left[\frac{d}{2} + h - \left(\frac{d}{2} \right)^2 \right] d\varphi \tag{2}$$

where ω represent the cutting angle, $\omega = \arccos \left(1 - \frac{2a_e}{d} \right)$; d is the milling tool diameter; φ is the cut-out angle.

Then, the relationship between shaded are S_{ABF} and chip contact area S_{ABG} can be obtained as

$$S_{ABG} = \frac{S_{ABF}}{\cos \left(\frac{\pi}{6} \right)} \tag{3}$$

The Johnson–Cook constitutive model, which takes into account the effects of strain hardening, strain state, and thermal softening, can be adopted to estimate the flow stress in the material. Thus, in the shear zone, the material flow stress can be calculated as [12]

$$\tau = (A + B * \varepsilon^n) \left[1 + C * \ln \left(\frac{\dot{\varepsilon}}{\dot{\varepsilon}_0} \right) \right] \left[1 - \left(\frac{T - T_r}{T_m - T_r} \right)^m \right] \tag{4}$$

where ε is the effective strain on the shear surface of the material; $\dot{\varepsilon}$ is the effective strain rate on the shear surface; $\dot{\varepsilon}_0$ is the reference plastic strain rate, usually $1S^{-1}$; A is the workpiece yield strength (MPa); B is the workpiece

Table 1 Johnson–Cook constitutive parameters of 45 steel [13]

A	B	C	n	m	$\dot{\epsilon}$	T_r	T_m
507MPa	320MPa	0.064	0.28	1.06	$1S^{-1}$	25 °C	1492 °C

harden-ing modulus (MPa); C is the sensitivity coefficient of the workpiece strain rate; n is the coefficient of workpiece hardening; m is the coefficient of workpiece softening; T is the instantaneous workpiece temperature (°C); T_r is the indoor temperature (°C); T_m is the melting temperature of the work-piece material (°C).

The workpiece material is assumed to be 45 steel and the cutter tool material is K-class cemented carbide. Johnson–Cook constitutive model parameters of 45 steel are listed in Table 1.

For a sharp tool, the chip forming force is equal to the cutting force [14]. Therefore, the chip forming force can be obtained by calculating the cutting force of the sharp tool. The shear force F_s is [15]

$$F_s = \frac{S * \tau}{\sin \phi} \quad (5)$$

where S is the contact area between the tool and the chip (m^2), τ is the material flow stress in the shear zone (MPa), and ϕ is the shear angle. The shear angle can be expressed as [16]

$$\phi = \frac{\pi}{4} + \frac{\gamma_0}{2} - \frac{\beta}{2} \quad (6)$$

Where γ_0 is the rake angle of the tool and β is the friction angle of the rake face. The friction angle β is related to the cutting speed and the friction coefficient [17].

The average friction coefficient f and the contact friction angle β between the chip and the tool are [17]

$$f = f_0 * V^p \quad (7)$$

$$\beta = \arctan(f) \quad (8)$$

where f_0 and p are constants, equal to 0.704 and -0.248, respectively; V is the cutting speed (m/min).

According to the fundamental principle of material removal by chip formation, the relationship between the force vectors involved in chip formation can be obtained, as shown in Fig. 1. Then, the cutting force components F_c and F_t can be calculated as

$$F_c = \frac{F_s * \cos(\beta - \gamma_0)}{\cos(\phi + \beta - \gamma_0)} \quad (9)$$

$$F_t = \frac{F_s * \sin(\beta - \gamma_0)}{\cos(\phi + \beta - \gamma_0)} \quad (10)$$

where F_c is the chip forming force component in the feed direction of the cutter and F_t is the chip forming force component perpendicular to the feed direction, both expressed in Newtons.

Plowing force model

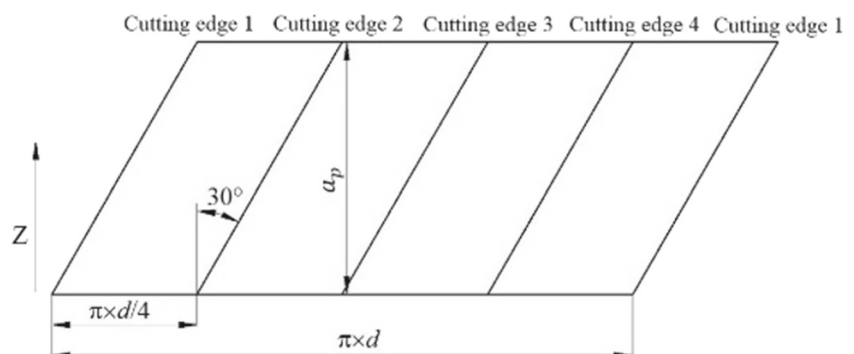
(1) Modeling of the tool-chip contact length

Due to the limitations of the milling process, the cutting edge of a micro end-mill cannot be considered perfectly sharp. Furthermore, the uncut chip thickness can be reduced to dimensions comparable with those of the tool edge radius; therefore, the plowing action will be more dominant.

Since milling is an intermittent cutting process, edge radius r_e and contact length b are important factors affecting the plowing force induced by the cutting edge in the milling process. Therefore, edge radius r_e and contact length b between the tool and the chip should be first obtained in order to solve the plowing force components. In the milling process, contact length b between the tool and the chip is related to the axial cutting depth a_p , spiral angle δ , and milling form. Taking semi-milling as an example, the formula for determining whether the cutting edge cuts the workpiece can be derived as

$$j = \begin{cases} 1 & k * \frac{\pi}{2} \leq \varphi_1 \leq k * \frac{\pi}{2} + \frac{2 * a_p}{\sqrt{3} * d} \\ 0 & k * \frac{\pi}{2} + \frac{2 * a_p}{\sqrt{3} * d} \leq \varphi_1 \leq (k + 1) * \frac{\pi}{2} \end{cases} \quad (11)$$

Where φ_1 is the rotation angle of the tool, $k = 0, 1, 2, 3$, a_p is the axial cutting depth, and d is the diameter of the milling tool. When $j = 1$, the corresponding value of d

Fig. 3 Axial expansion of spiral milling tool

indicates that a cutting edge exists that cuts the workpiece. When $j = 0$, the corresponding value of d indicates that no part of the cutting edge cuts the workpiece.

When a cutting edge cuts the workpiece, a relationship can be established between the axial cutting depth a_p and the contact length b between the tool and the chip. According to Fig. 3, the contact length between the tool and the chip can be expressed as

$$b = \begin{cases} \frac{2\sqrt{3}a_p}{3} & Z = 1 \\ \frac{\pi d^3}{2} & Z > 1 \end{cases} \quad (12)$$

Where a_p is the axial cutting depth and d is the diameter of milling tool.

(2) Cutting layer parameters of edge preparation

As shown in Fig. 1, the plowing force can be calculated using the Waldorf slip-line field model. Angle ρ of the connection area between the chip and the uncut layer is 10

degrees [18]. The friction condition η on the CA surface can be expressed as [19]

$$\eta = 0.58 * \arcs(m_1) \quad (13)$$

where m_1 is the friction coefficient of the dead-metal zone, usually 0.8.

Radius R of the fan field can be solved according to the relation between the edge radius r_e and the fan field, as shown in Fig. 1. Angles θ and ξ are calculated based on their relationship, as follows [19]:

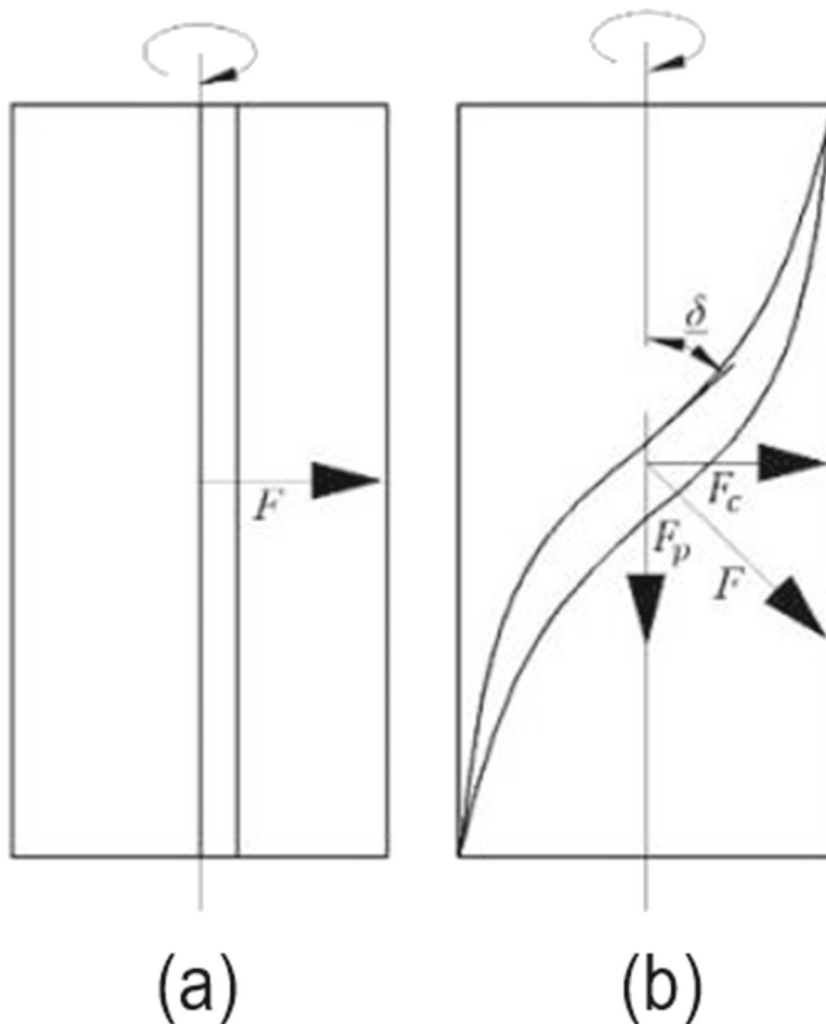
$$R = \sin \eta * \sqrt{\left[r_e * \tan\left(\frac{\pi}{4} + \frac{\gamma_0}{2}\right) + \frac{\sqrt{2} * \sin \rho}{\tan\left(\frac{\pi}{4} + \frac{\gamma_0}{2}\right)} \right]^2 + 2 * (R * \sin \rho)^2} \quad (14)$$

$$\theta = \frac{\pi}{4} - \rho - \phi \quad (15)$$

$$\xi = \eta + \phi - \arcsin(\sqrt{2} * \sin \rho * \sin \eta) \quad (16)$$

where r_e is the edge radius.

Fig. 4 Schematic illustration of milling tool: (a) No helix angle; (b) With helix angle



(3) Establishment of plowing force component model

The plowing force component P_c in the tool feed direction and the plowing force component P_t perpendicular to the tool feed direction are

$$P_c = \frac{R}{\sin \eta} * \tau * b[(1 + 2 * \xi + 2 * \theta + 2 * \sin(2 * \eta)) * \sin(\phi - \xi + \eta) + \cos(2 * \eta) * \cos(\phi - \xi + \eta)] \quad (17)$$

$$P_t = \frac{R}{\sin \eta} * \tau * b[(1 + 2 * \xi + 2 * \theta + 2 * \sin(2 * \eta)) * \cos(\phi - \xi + \eta) + \cos(2 * \eta) * \sin(\phi - \xi + \eta)] \quad (18)$$

where b is the contact length between the tool and the chip.

Cutting force model

From Fig. 1, it can be observed that the total cutting force F_C in the feed direction of the milling tool is composed of the chip forming force component F_c in the feed direction and the plough cutting force component P_c in the feed direction. The total cutting force F_T perpendicular to the feed direction is composed of the chip forming force component F_t perpendicular to the tool feed direction and plough cutting force component P_t perpendicular to the feed direction.

Therefore, the cutting force components of the edge prepared milling tool can be expressed as

$$F_C = F_c + P_c \quad (19)$$

$$F_T = F_t + P_t \quad (20)$$

The relationship between the axial cutting force F_P and cutting force F_C in the tool feed direction is shown in Fig. 4.

From Fig. 4 (b), the axial cutting force F_P is

$$F_P = F_C * \tan \delta \quad (21)$$

where δ is the spiral angle.

Based on the obtained total cutting force in the tool feed direction, perpendicular to the tool feed direction, and in the axial direction, the formula for converting the total cutting force into the workpiece coordinates in the X , Y , and Z directions is

$$\begin{bmatrix} F_x \\ F_y \\ F_z \end{bmatrix} = K \begin{bmatrix} F_C \\ F_T \\ F_P \end{bmatrix} \quad (22)$$

where K is the conversion factor. The coefficient can be solved using a system of equations.

A flowchart of the parameter identification process of the micro end-milling cutting force model is shown in Fig. 5.

Milling Process Simulations

Simulations of the milling were used to verify the cutting force model. The simulation model was established in

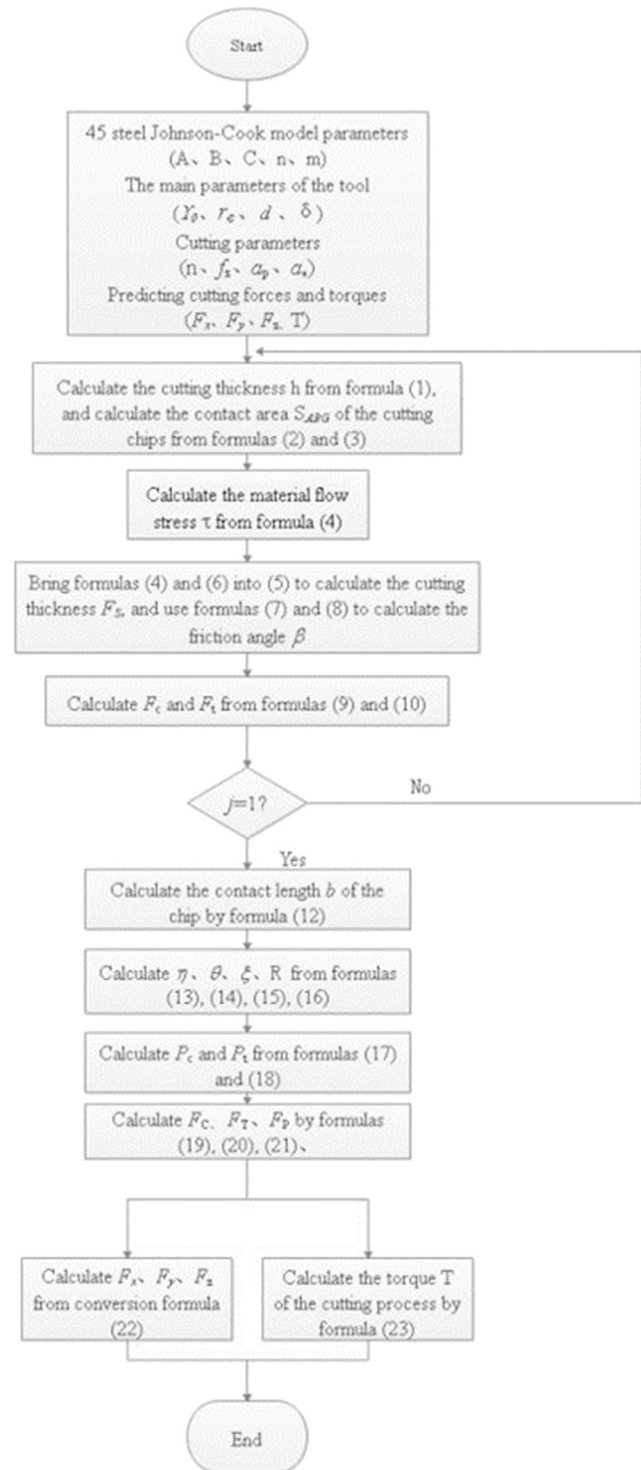
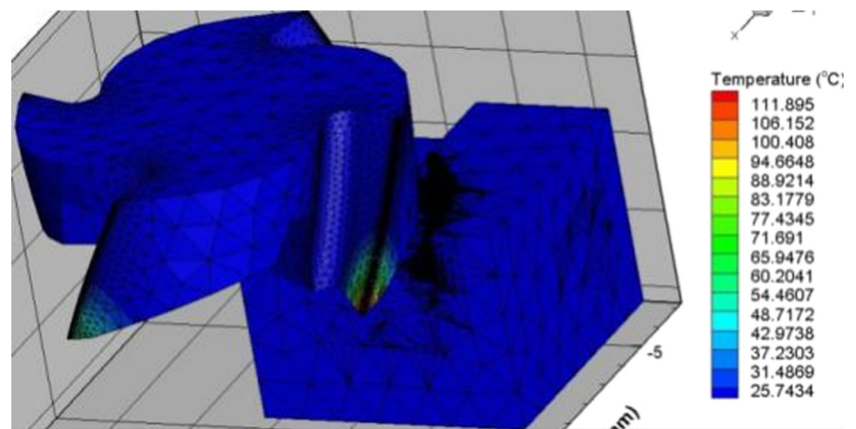


Fig. 5 Flowchart of parameter identification process of micro end-milling cutting force model

AdvantEdge, a simulation and analysis software based on the FEM, as shown in Fig. 6. The AdvantEdge software is often used to analyze cutting, forming, and heat treatment processes. Cutting tool properties and cutting process



Fig. 6 Finite element model of milling process



parameters can be optimized through simulations, which effectively remove the cost of performing experiments.

For the simulations, corner milling with down milling was adopted. Three-dimensional (3D) models of the cutting tool with different edge radiuses and the workpiece were established in SolidWorks. The cutting tool was a cemented carbide end milling tool (ZX40). The tool geometry and material properties are presented in Table 2. The workpiece as 45 steel in an annealed state with dimensions of 160*100*50mm.

The friction coefficient was set as 0.8, the initial temperature was 25 °C, and the rotation angle was 90°. Selecting the appropriate constitutive equations is the key to realizing accurate cutting simulations. The Johnson–Cook model takes into account the effects of different factors, such as strain, strain rate, and thermal softening on the hardening stress of materials, and is particularly well suited to simulating metal materials at high strain rates; therefore, the Johnson–Cook constitutive equation is also referred to as the flow stress equation. To balance simulation speed and accuracy, the minimum mesh value of the tool was set to 1/3 of the edge radius. A coarse mesh was used farther away from the cutting edge, while a finer mesh was applied close to the cutting edge.

The main parameters of the milling process that were used to evaluate the influence of cutting edge preparation on the cutting force are the edge radius r_e , milling speed, cutter tool feed rate, cutting depth, and rake angle. The specific

milling parameter values used in simulations are presented in Table 3.

Milling Process Experiment

To validate the theoretical model proposed in this paper, theoretical cutting torque values were compared to experimental measurements. During the milling process, the cutting parameters and edge radius will affect cutting performance. Therefore, orthogonal experiments were designed to accurately reflect the influence of the cutting parameters and edge radius on cutting performance. The drag finishing method was used to edge prepare the cemented carbide tool, as shown in Fig. 7, and the tools with different asymmetric cutting edges were obtained and used to perform milling experiments on a 45 steel workpiece.

The drag finishing method can be used as both the edge preparation process and workpiece polishing. Dispersed solid abrasives, including walnut powder, brown corundum particles, and silicon carbide particles mixed at a certain ratio, were packed into a container. The tool was then installed on the spindle and passed through the abrasive particles along a two-stage planetary trajectory. This method can realize both rotational and the revolution movements of a single tool, as well as a group of tools. The tool edge is prepared by continuous impacts from dispersed solid abrasive particles, which remove micro defects, thereby realizing efficient and uniform edge preparation.

Table 2 Tool geometry and material properties

Rake angle	Relief angle	Edge length (mm)	Total Length (mm)	Rolling friction coefficient
14°	15°	25	75	0.01
Poisson's ratio	Shear modulus (Pa)	Density (Kg/m3)	Diameter (mm)	
0.3	2.63×10^{11}	1456	10	



Table 3 Conditions used in milling simulations

number	Speed (r/min)	Feed (mm/Z)	Cutting Depth (mm)	Rake angle (°)	Edge radius (μm)
1	2300	0.13	0.8	19	11.8
2	2300	0.13	0.8	17	11.8
3	2300	0.13	0.8	15	11.8
4	2300	0.13	0.8	14	11.8
5	2300	0.13	0.8	11	11.8
6	2300	0.13	0.8	10	11.8
7	2300	0.1	0.8	14	11.8
8	2300	0.11	0.8	14	11.8
9	2300	0.17	0.8	14	11.8
10	2300	0.13	0.8	14	7.1
11	2300	0.13	0.8	14	17.7
12	3000	0.25	1.0	14	27.0
13	2300	0.13	0.8	14	35.3
14	2000	0.17	1.2	14	17.7
15	2100	0.17	1.2	14	17.7
16	2300	0.17	1.2	14	17.7
17	2700	0.17	1.2	14	17.7
18	2000	0.1	0.5	14	7.1

Since movements of the dispersed solid abrasive particles are random, this complex behavior is difficult to model, and further studies on the edge preparation process are still needed. Following the edge preparation process, asymmetric edge morphologies of the cutter were analyzed using the Infinite Focus SL optical 3D measurement system, as shown in Fig. 8.

A horizontal three-axis milling vertical machining center (KMC800V) was used to perform the required experiments using the following parameters: travel range of 800 mm, 650 mm, and 450 mm along the x , y , and z axes, respectively; maximum torque of 62 N·m; maximum feed speed of 48 m/min and 60 m/min, along the x and y axis, respectively; maximum speed of 16000 rpm; positioning accuracy of 8.5 μm . The cutting force was measured with a Spike® wireless dynamic cutting dynamometer installed inside the tool handle or spindle, which can directly and wirelessly detect the cutting force and torque. The main components of the cutting force detection system included a HSK63 wireless induction knife handle, Spike receiver, computer, and data acquisition software (Spike Tool Measurement 2016 EN). The cutting forces were processed and analyzed in the data analysis software of the dynamometer (Spike Tool Analyzer, 2016). The KMC800 V three-axis milling vertical machining center is shown in Fig. 9. Parameters used in the milling experiments are presented in Table 4.

**Fig. 7** Photograph of drag finishing machine

Results and Analysis

Comparison of Theoretical and Simulated Cutting Forces

To verify the theoretical model, cutting forces, F_x , F_y , F_z and , were calculated using the proposed model and compared with simulated values, as shown in Fig. 10. For all milling conditions, good agreement between the numerical and simulation results was observed.

Figure 10(a) shows that the trend of cutting force from the theoretical model is the same as the simulation results. The minimum and maximum relative errors were 0.6% and 23.2%, respectively, except for group 13, the error was more than 20%, the others were less than 20%, and the mean error of all groups was 8.89%, suggesting that ignoring the end edge does not greatly affect the cutting force F_x . Similarly, the trends of cutting force F_y from the model and simulations were similar, as shown in Fig. 10(b), and the total error is small. The trends of cutting force F_z produced by the theoretical model and simulation are the same, as shown Fig. 10(c), however, the simulated values are smaller. In this paper, the edge only considers the circumference edge in the theoretical force model.

Fig. 8 Infinite Focus SL optical 3D measurement system



Fig. 9 Photographs of the KMC800 V three-axis milling vertical machining center

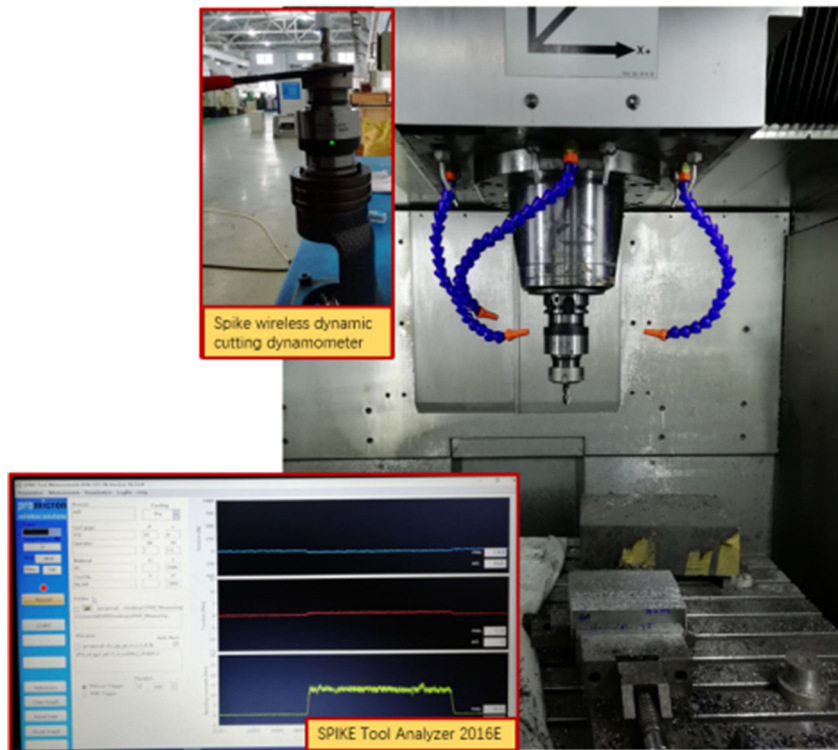


Table 4 Experimental milling conditions

number	Edge radius (µm)	Feed (mm/Z)	Speed (r/min)	a_p (mm)	a_e (mm)
1	5.40	0.12	800	1.6	1.7
2	5.40	0.16	1600	2.8	1.0
3	5.40	0.08	2400	2.2	3.1
4	6.20	0.16	2400	2.8	1.7
5	6.50	0.08	3200	2.8	1.7
6	6.20	0.12	3200	2.2	1.0

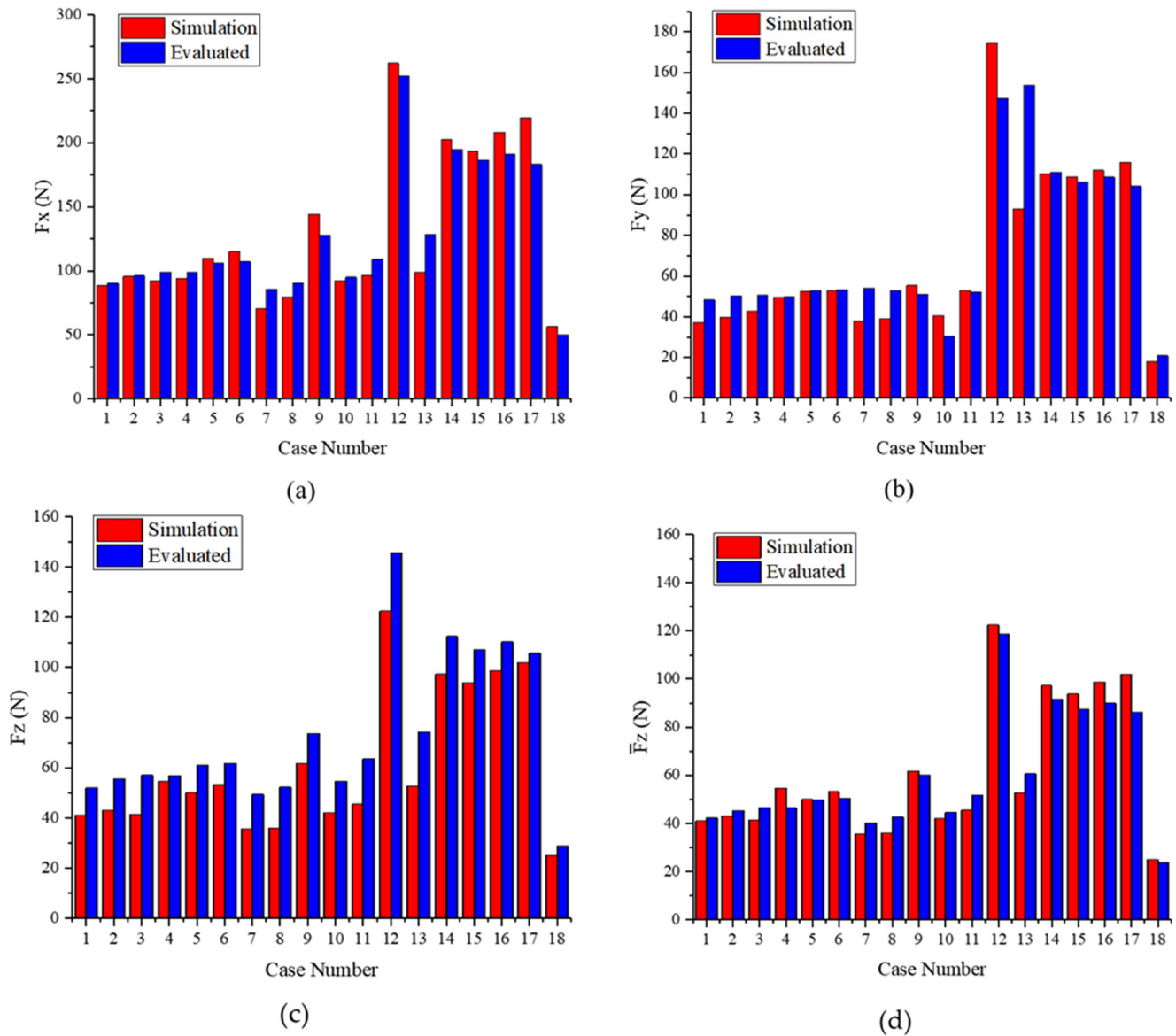


Fig. 10 Comparison of theoretical and simulated cutting force values: (a) Cutting force F_x ; (b) Cutting force F_y ; (c) Cutting force F_z ; (d) Cutting force \bar{F}_z ;

However, in the simulation cutting process, the milling tool end face is affected by the reaction force of the machined surfaces. Therefore, the simulated values of cutting force F_z decreased. So, the simulated values of cutting force F_z is lower than the evaluated.

In fact, this model presents regular errors due to simplified conditions, which is common in the process of cutting force modeling. For example, Kang et al. [20] introduced dimensionless compensation coefficient to compensate for the errors caused by material characteristics. In this paper, the correction coefficient is also introduced to reduce the model error.

$$\bar{F}_z = \zeta F_z \quad (23)$$

In equation (23), ζ is the average value of experimental correction coefficient of each group, taking 0.816. The corrected cutting force and simulation value are shown in Fig. 10(d). It can be seen from the figure that the error between the model and simulation is small, the minimum error is 0.11% and the maximum error is 15.22%, so the corrected model is effective.

Influence of Edge Radius and Cutting Parameters on Cutting Force

The influence of edge radius r_e and cutting parameters on the cutting force are illustrated in Figs. 11, 12, 13 and 14. From Fig. 11, it can be observed that as the edge radius



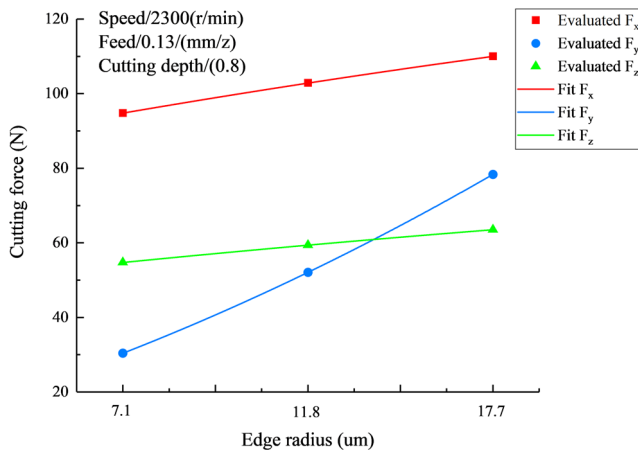


Fig. 11 Variation of cutting force with edge radius

r_e increases, the cutting force increases. When edge radius r_e is large and increasing, the strain and temperature of the processing surface also increase. A larger cutting force is needed to cut the material, therefore, the cutting force increases with the edge radius. Cutting force F_y increases more significantly than F_x and F_z with the increasing edge radius. As shown in Fig. 12, the cutting force gradually increases as the rake angle decreases, and F_x significantly increases. As the rake angle decreases from 19° to 10° , F_x increases by about 19%, while F_y and F_z increase only slightly. Figure 13 shows that the cutting force decreases slowly with the increasing milling speed. In addition, as the feed per tooth increases, the cutting force tends to increase, as shown in Fig. 14. Growth of the cutting area causes an increase in the cutting force, however, the effect on F_x is more significant, compared to F_y and F_z . When the feed per tooth increases from 0.10 mm/z to 0.17 mm/z, F_x approximately doubles.

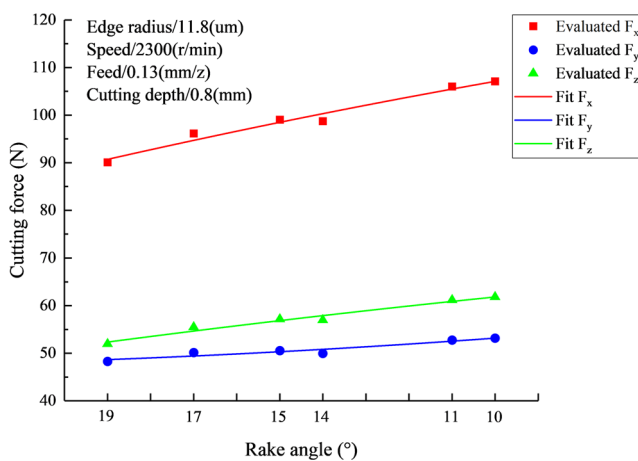


Fig. 12 Variation of cutting force with milling rake angle

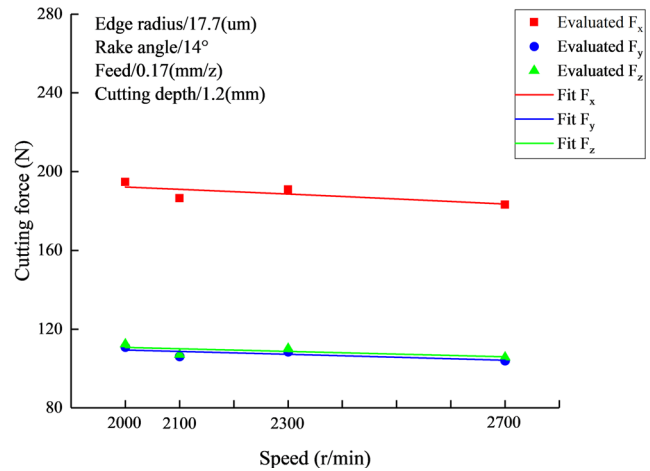


Fig. 13 Variation of cutting force with milling speed

Comparison of Theoretical and Experimental Cutting Torque

The milling tool torque can be expressed in terms of the total cutting force F_C and milling tool diameter d as

$$T = F_C * \frac{d}{2} \tag{24}$$

A comparison of the theoretical and experimental values of torque is presented in Fig. 15, and similar trends can be observed. The minimum error is 1.1% and the maximum error is 21%. Similar to “Comparison of Theoretical and Simulated Cutting Forces”, except for the second group, the error is more than 20%, the rest are less than 20%, and the mean error of all groups is 13.12%. The experimental results show that the theoretical model of cutting force can accurately predict torque in the milling process using an edge prepared milling tool.

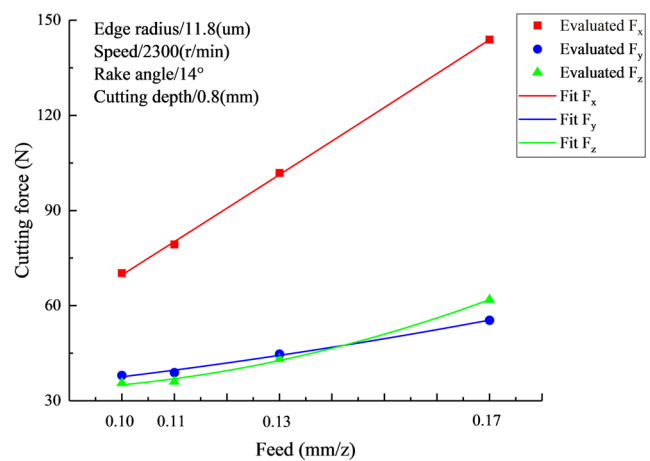


Fig. 14 Variation of cutting force with tool feed



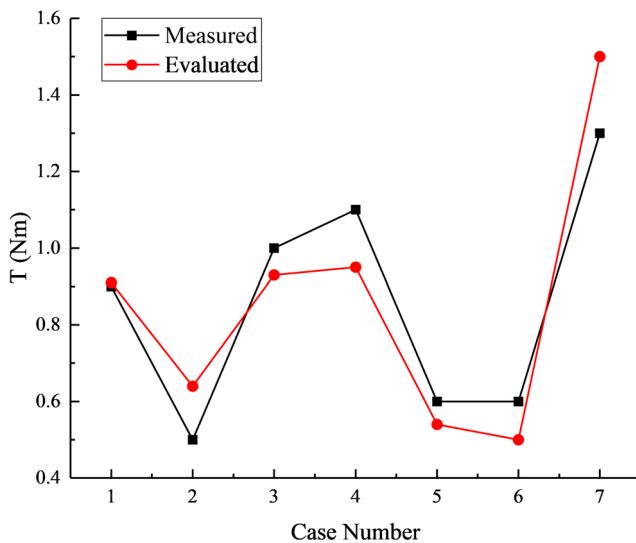


Fig. 15 Comparison of theoretical and experimental values of torque

Conclusion

This paper presented a novel micro end-milling force model derived using material constitutive equations, metal cutting theory, and slip-line theory. The established cutting force model considering cutting edge preparation was verified through simulations and validated by experiment. The main conclusions can be summarized as follows:

- (1) The edge radius can significantly affect the micro end-milling process. Predicted cutting forces increase with increasing cutting edge radius. Cutting force component F_y increases more significantly than F_x and F_z as the edge radius increases.
- (2) The variation of cutting force F_x observed using the proposed theoretical model is similar to the trend in simulated values, with a minimum error is 0.6% and the mean error is 8.89%. Ignoring the cutting force solution of the end edge has no obvious effect on F_x . The theoretical and simulated cutting force F_y is similar, and the total error is small.
- (3) The variation of cutting force F_z observed using the theoretical model is similar to the observed trend of simulated values, however, the simulation results are smaller. This is likely because the effect of the end edge on cutting force is ignored in the theoretical modeling process, which could lead to larger values of the axial cutting force component F_p . By introducing the correction coefficient, the prediction error can be kept below 15.22%.
- (4) The variation of torque observed in the theoretical results is the same as the trend of torque values measured in milling experiments, with a minimum error of 1.1% and mean error of 13.12%. The

results show that the theoretical model can accurately calculate the torque of milling tools with different edge radiuses.

Author Contributions Xuefeng ZHAO: Graduate tutors, put forward research topics; Design the research plan; Obtaining research funding; Yong YANG: Master's degree student and Research and organize literature; Design the framework of the thesis; Draft papers; Revise the thesis;

Lin He: Supervisor of the master degree dissertation;

Zhiguo Feng: Supervisor of the master degree dissertation.

Funding This work is supported by the National Natural Science Foundation of China. (Research on the influence of tool passivation and asymmetric cutting edge on cutting performance), China.

Nomenclature F_s , Shear force; F_C , Cutting force in the tool feed direction; F_p , Axial cutting force; h , Cutting thickness; a_e , Radial cutting depth; a_p , Cutting depth; δ , Spiral angle; f_z , Feed engagement; φ , Cut-out angle; ω , Cutting angle; d , Milling tool diameter; γ_0 , Rake angle; β , Friction angle of the rake face; ϕ , Shear angle; V , Cutting speed; b , Contact length between the tool and the chip; τ , Material flow stress in the shear zone; ρ , Angle between the chip and the uncut layer.

References

1. Bernhard K, Schmidta K, Beñob J (2014) Measuring procedures of cutting edge preparation when hard turning with coated ceramics tool inserts. Measurement 55:627–640
2. Denkena B, Biermann D (2014) Cutting edge geometries. CIRP Ann Manuf Technol 63(2):631–653
3. Bouzakis K, Bouzakis E, Kombogiannis S, Makrimalakis S, Skordaris G, Michailidis N, Charalampous P, Paraskevopou-lou R, M'Saoubi R, Aurich J (2014) Effect of cutting edge preparation of coated tools on their performance in milling various materials. CIRP J Manuf Sci Technol 7:264–73
4. Rubeo MA, Schmitz TL (2016) Milling force modeling: a comparison of two approaches[J]. Procedia Manuf 5:90–105
5. Weng J, Zhuang K, Hug C (2020) A PSO-based semi-analytical force prediction model for chamfered carbide tools considering different material flow state caused by edge geometry. Int J Mech Sci, 1691
6. Magalhães FC, Ventura CEH, Abrão AM, Denkena B (2020) Experimental and numerical analysis of hard turning with multi-chamfered cutting edges. J Manuf Process 49:126–134
7. Agmell M, Ahadi A, Gutnichenko O, Stahl J-E (2017) The influence of tool micro-geometry on stress distribution in turning operations of AISI 4140 by FE analysis. Int J Adv Manuf Technol 89:3109–22
8. Zhou L, Peng F, Yan R, Yao P, Yang C, Li B (2015) Analytical modeling and experimental validation of micro end-milling cutting forces considering edge radius and material strength-ening effects. Int J Mach Tool Manu 97:29–41
9. Fulemova J, Janda Z (2014) Influence of the cutting edge radius and the cutting edge preparation on tool life and cutting forces at inserts with wiper geometry. Procedia Eng 69:565–573
10. Wang F, Yin J, Ma J et al (2017) Effects of cutting edge radius and fiber cutting angle on the cutting-induced surface damage in machining of unidirectional CFRP composite laminates. Int J Adv Manuf Technol 91:3107–3120
11. Zhu K, Li K, Mei T et al (2016) Research progress in micro-milling force modeling[J]. J Mech Eng 52(17):20–30



12. Sauer K, Witt M, Putz M (2019) Influence of cutting edge radius on process forces in orthogonal machining of carbon fibre reinforced plastics (CFRP). *Procedia CIRP* 85:218–223
13. Denkena B, Vehmeyer J, Niederwestberg D, Maaß P (2014) Identification of the specific cutting force for geometrically defined cutting edges and varying cutting conditions. *Int J Mach Tools Manuf* 82-83:42–9
14. Denkena B, Lucas A, Bassett E (2011) Effects of the cutting edge microgeometry on tool wear and its thermo-mechanical load. *CIRP Ann* 60:73–6
15. Oxley PLB, Young HT (1990) *The mechanics of machining: an analytical approach to assessing machinability*[J]. Ellis Horwood Publisher, Chichester, England
16. Merchant ME (1945) Mechanics of the metal cutting process[J]. I. Orthogonal cutting and a type 2 chip. *J Appl Phys* (16):267–275
17. Dudzinski D, Molinari A (1997) A modelling of cutting for visco-plastic materials[J]. *Int J Mech Sci* (39):369–389
18. Su JC (2006) *Residual stress modeling in machining processes*[J]. Georgia Institute of Technology
19. Waldorf DJ, DeVor RE, Kapoor SG (1998) A slip-line field for ploughing during orthogonal cutting[J]. *J Manuf Sci Eng* (120):693–699
20. Kang IS, Kim JS, Kim JH, Kang MC, Seo YW (2006) A mechanistic model of cutting force in the micro end milling process[J]. *J Mater Process Tech* 187

Publisher's Note Springer Nature remains neutral with regard to jurisdictional claims in published maps and institutional affiliations.

